

CERTIFICATE

It is certified that the work contained in the thesis titled **“Phase Evolution, Thermal Stability and Mechanical Properties of Some Low-density High Entropy Alloys”** by Nandini Singh has been carried out under my supervision and that this work has not been submitted elsewhere for a degree.

It is further certified that the student has fulfilled all the requirements of Comprehensive, Candidacy and SOTA for the award of Ph.D. degree.



Prof. N.K.Mukhopadhyay
(Supervisor)
Department of Metallurgical Engineering
Indian Institute of Technology
(Banaras Hindu University)
Varanasi

DECLARATION BY THE CANDIDATE

I, Nandini Singh, certify that the work embodied in this Ph.D. thesis is my own bonafide work carried out by me under the supervision of Prof. N. K. Mukhopadhyay for a period from December 2013 to December 2021 at the Department of Metallurgical Engineering, Indian Institute of Technology (BHU), Varanasi. The matter embodied in this Ph.D. thesis has not been submitted for the award of any other degree/diploma. I declare that I have faithfully acknowledged and given credits to the research workers wherever their works have been cited in my work in this thesis. I further declare that I have not wilfully copied any other's work, paragraphs, text, data, results, *etc.*, reported in journals, books, magazines, reports dissertations, thesis, *etc.*, or available at websites and have not included them in this thesis and have not cited as my own work.

Date: 06.12.2021

Nandini Singh

Place: Varanasi

(Nandini Singh)

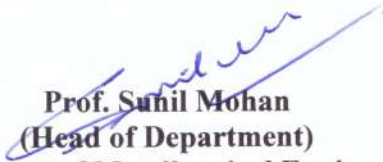
CERTIFICATE BY THE SUPERVISOR

This is to certify that the above statement made by the candidate is correct to the best of my knowledge.



Prof. N.K. Mukhopadhyay
(Supervisor)
Department of Metallurgical Engineering
Indian Institute of Technology
(Banaras Hindu University)
Varanasi

Forwarded by



Prof. Sunil Mohan
(Head of Department)
Department of Metallurgical Engineering
Indian Institute of Technology
(Banaras Hindu University)
Varanasi

COPYRIGHT TRANSFER CERTIFICATE

Title of the Thesis: Phase Evolution, Thermal Stability and Mechanical Properties of Some Low-density High Entropy Alloys.

Candidate's Name: Nandini Singh

Copyright Transfer

The undersigned hereby assigns to the Indian Institute of Technology (Banaras Hindu University), Varanasi all rights under copyright that may exist in and for the above thesis submitted for the award of the *Doctor of Philosophy*.

Date: 06.12.2021



Place: Varanasi

(Nandini Singh)

Note: However, the author may reproduce or authorize others to reproduce materials extracted verbatim from the thesis or derivative of the thesis for author's personal use provided that the source and the Institute's copyright notice are indicated.

ACKNOWLEDGEMENT

Before I start, I would like to thank, the Almighty for guiding me through the years of my studies and giving me all strength required to sustain the days of hardship. I also bow in gratitude to Almighty to have given me an opportunity to study in the Indian Institute of Technology (Banaras Hindu University) founded by visionary legend Mahamana Pandit Madan Mohan Malaviya.

I will take this opportunity to express my sincere thanks and gratitude to my supervisor Prof. N. K. Mukhopadhyay for his consistent guidance and encouragement during the entire duration of Ph.D. work. His immense support has helped to sail through difficult times encountered in last eight years. Besides my advisors, I would like to thank the rest of my RPEC members: Prof. P. Maiti (SMST) and Prof. B. N. Sarma for their support and insightful comments.

I would like to convey my sincere thanks to Prof. Sunil Mohan, Head of Department and former Heads, Prof. N. K. Mukhopadhyay, Prof. R. K. Mandal and Prof. G. V. S. Sastry for their valuable comments, suggestions and needful help extended for conducting my research work.

I express my sincere thanks to entire faculty members of the department for their valuable suggestions. I will like to acknowledge the Dr. Rampada Manna (Coordinator, ARCIS) and Prof. Rajiv Prakash (CIF, IIT (BHU)) for extending necessary characterization facility. My sincere thanks to Mr. Lalit Kumar Singh for his invaluable help extended during TEM investigation and Mr. Girish Sahu (CIF, IIT (BHU)) for his constant help in conducting SEM studies.

My sincere thanks to Mr. Kamala Prasad, Mr. J P Patel, Mr. Arun Prakash, Mr. Rana Pratap Yadav, Mr. Chotey Lal, Mr. Rajendra Yadav and Mr. Anjani and all the non-teaching staffs of department. I thankfully acknowledge help of my seniors Drs. Manish, Deepa, Rajbhadrur, my fellow colleagues Drs Vikas Shivam, Vivek Kumar Pandey and Yagnesh Shadangi and other fellow labmates Harsh Jain, Priyatosh Pradhan and Rajat Gupta.

A special thanks to my family. Words cannot express their sacrifices they have made for me. Their support, moral and spiritual guidance has helped me overcoming difficult situations. Last but not the least, I am thankful to all those who have helped me throughout this period, but unwillingly I could not mention them.

Nandini Singh

(Nandini Singh)

Table of Contents

List of Figures	xi
List of Tables	xiv
Abbreviations	xv
Symbols.....	xvi
Preface	xvii
CHAPTER 1: Introduction and Literature Review	1
1.1. Historical Preview	1
1.2. High Entropy Alloys	2
1.2.1 Principle of high entropy alloys	3
1.2.2. Classification on the basis of configurational entropy.....	4
1.2.3. The Four Core Effects.....	5
1.2.4. Phase Prediction Rules in HEAs.....	10
1.3. Synthesis and Processing Routes for HEAs.....	12
1.3.1 Vacuum Arc Melting (VAR)	13
1.3.2. Vacuum induction melting (VIM)	13
1.3.3. Mechanical Alloying (MA).....	14
1.3.4. Spark Plasma Sintering (SPS)	16
1.3.5. Other consolidation techniques.....	17
1.3.6. Thin Films of HEAs	17
1.4. Important Classes of HEAs	18
1.4.1. Solid-Solutions.....	18
1.4.2. Low-density HEAs (LDHEAs).....	23
1.5. Thermal stability	24
1.6. Properties of HEAs	25
1.6.1. Mechanical Behavior of HEAs	25
1.6.2. Physical Behavior	31
1.7. Miedema's model: A Semi - empirical approach	32
1.8. CALPHAD: Phase Diagram Approach	33
1.9. Prospective Applications of HEAs	34
1.10. Motivation.....	35
1.11. Objectives	36

CHAPTER 2: Materials and Experimental Details	37
2.1. Materials and Alloy Synthesis	37
2.2. Spark Plasma Sintering of HEA Powder	39
2.3. Density Measurement	39
2.4. Structural Characterization	39
2.4.1. X-ray diffraction (XRD)	39
2.4.2. Scanning Electron Microscopy (SEM)	40
2.4.3. Transmission Electron Microscopy (TEM)	41
2.5. Thermal Analysis	41
2.5.1. Differential Scanning Calorimetry (DSC)	41
2.5.2. Heat treatments	42
2.6. Mechanical testing	42
2.6.1. Hardness measurement	42
2.7. CALPHAD approaches.....	42
CHAPTER 3: Phase evolution and thermal stability of MgAlSiCrFe low-density high entropy alloy processed through mechanical alloying and spark plasma sintering	43
3.1. Alloying behavior and phase evolution of milled MgAlSiCrFe HEA powder	43
3.2. Phase analysis and mechanical properties of the SPSed MgAlSiCrFe HEA.....	52
3.3. Discussion	57
3.4. Conclusions.....	69
CHAPTER 4: Phase evolution, thermal stability and indentation behavior of MgAlSiCrFeNi low-density high entropy alloy processed through mechanical alloying and spark plasma sintering	71
4.1. XRD analysis of MgAlSiCrFeNi high entropy alloy.....	71
4.2. Nanostructured nature and powder morphology of milled powder	74
4.3. Thermal stability of the milled powder	78
4.4. Consolidation and microstructural evolution of MgAlSiCrFeNi HEA	83
4.5. Mechanical Behavior of MgAlSiCrFeNi HEA	87
4.6. Discussion	89
4.7. Conclusions.....	95

CHAPTER 5: Phase evolution, thermal stability and indentation behavior of MgAlSiCrFeCuZn low-density high entropy alloy processed through mechanical alloying and spark plasma sintering	97
5.1. Phase evolution during mechanical alloying of MgAlSiCrFeCuZn powder	97
5.2. Nanostructure nature and elemental mapping of mechanically alloyed powder	103
5.3. Analysis of powder morphology and thermal stability of the milled powder	108
5.4. Phase evolution and mechanical properties of the SPSed LDHEA.....	110
5.5. Discussion	111
5.6. Conclusions	114
CHAPTER 6: SUMMARY AND SUGGESTIONS FOR FUTURE WORK	115
6.1. Summary	115
6.2. Suggestions for future work.....	117
REFERENCES.....	119
LIST OF PUBLICATIONS & CONFERENCE PRESENTATIONS.....	129

List of Figures

		<i>Page No.</i>
Figure 1.1	Timeline for the development of materials.....	2
Figure 1.2	The depicted notion of random mixing of components in a multi-component alloy, as indicated by the circles in various colors. With equal atom sizes and loose atomic packing implied, the configuration entropy of mixing the alloy is identical to that of an ideal gas, and so is maximized by the use of an equiatomic composition design.....	7
Figure 1.3	Demonstrates the relationship among the parameters δ and Ω for multi-component alloys. Here "Solid Solutions" implies that the alloy is composed entirely of solid solution; "Intermetallics" demonstrates that the alloy is composed primarily of intermetallic compounds and other ordered phases; "S+I" implies that in multi-component alloys, not only solid solution but also ordered compounds can precipitate; and "BMGs" implies that the alloy is composed entirely of amorphous phase.....	12
Figure 1.4	Variation of hardness (HV) and crack length around the indent by varying the Al concentration in the $Al_xCoCrCuNiFe$ alloy system.....	26
Figure 3.1	Phase evolution after 60 h of mechanical alloying MgAlSiCrFe HEA powder (a); SEM micrograph showing the the morphology of 60 h milled powder scanned for elemental analysis (b); (c) SEM micrograph 60h milled powder; (d) EDS-Spectrum showing the presence of alloying element and elemental composition after 60 h of milling.....	44
Figure 3.2	TEM micrograph showing (a) bright-field image; (b) corresponding SAD pattern; (c) dark-field image of MgAlSiCrFe HEA powder milled for 60 h.....	46
Figure 3.3	STEM – EDS mapping of equiatomic MgAlSiCrFe LDHEA powder milled for 60 h (a) showing homogenous elemental distribution; (b) showing presence of homogenous elemental distribution of apart from Si.....	47
Figure 3.4	DSC thermogram of MgAlSiCrFe high entropy alloy powder milled for 60 h upto 1200 °C (1473 K).....	48
Figure 3.5	Sequence of phase evolution during isothermal heating from room temperature to 700 °C (973 K) for 60 h milled MgAlSiCrFe HEA.....	49
Figure 3.6	Exploded XRD plot showing the evolution of phases along with (110) reflection of BCC (Fe-based) and B2 (AlFe) type phase at (a) 600 °C (873 K) and (c) 700 °C	

	(973 K) respectively. Deconvolution of peaks showing presence of BCC (Fe-based), B2 (AlFe) and Al ₁₃ Fe ₄ phase at (b) 600 °C (873 K) and (d) 700 °C (973 K) respectively.....	50
Figure 3.7	TEM micrograph showing (a) bright-field image; (b) corresponding SAD pattern; (c) dark-field image of MgAlSiCrFe HEA powder milled for 60 h followed by annealing at 700 °C (973 K)	51
Figure 3.8	Phase evolution during spark plasma sintering of MgAlSiCrFe HEA at 800 °C (1073 K) (a); exploded image showing formation of minor phases along with the (110) peak of major phase (b); deconvolution showing the presence of minor Al ₁₃ Fe ₄ phase with major BCC/ B2 phase (c).....	53
Figure 3.9	BSE-SEM micrograph showing the microstructure of MgAlSiCrFe HEA spark plasma sintered at 800 °C (1073 K). (a) microstructure at low magnification; (b) microstructure showing fine distribution of phases; (c) microstructure scanned for full area elemental mapping; (d) microstructure showing the spots for point SEM-EDS analysis; (e) EDS spectrum showing presence of alloying elements.....	54
Figure 3.10	SEM-EDS mapping showing elemental distribution of MgAlSiCrFe HEA spark plasma sintered at 800 °C (1073 K)	57
Figure 3.11	Binary phase diagrams (binary subsystems of MgAlSiCrFe HEA) calculated by Thermo-Calc (SSOL5 database)	62
Figure 3.12	Property diagram of MgAlSiCrFe HEA using Thermo-Calc.....	66
Figure 4.1	Phase evolution during mechanical alloying of MgAlSiCrFeNi HEA powder upto 60 h.....	72
Figure 4.2	TEM micrograph showing (a, d) bright field image and (b, e) selected area diffraction pattern and (c, f) dark field image of LDHEA powder milled for 60 h showing presence of BCC along with minor fraction of Si.....	75
Figure 4.3	STEM-EDS mapping of equiatomic MgAlSiCrFeNi high entropy alloy mechanically alloyed for 60h showing elemental distribution.....	76
Figure 4.4	Morphology of MgAlSiCrFeNi HEA powder mechanically milled for (a) 10 h; (b) 20 h; (c) 30 h; (d) 50 h.....	77
Figure 4.5	DSC thermogram of MgAlSiCrFeNi HEA powder milled for 60 h showing exothermic and endothermic heating events.....	79

Figure 4.6	(a) Phase evolution during annealing of 60 h milled MgAlSiCrFe HEA powder upto 800 °C (1073K); (b) blown-up image for (110) peak of BCC phase showing evolution of other phases.....	81
Figure 4.7	TEM micrograph showing (a) bright field image and (b) selected area diffraction patterns and (c) dark field images of MgAlSiCrFeNi LDHEA annealed powder at 800 °C (1073K) for 60 min.	82
Figure 4.8	Phase formation in MgAlSiCrFeNi HEA powder spark plasma sintered at 800 °C (1073K) for 15 min (a); Blown-up image showing BCC/B2 phase along with other minor phases (b); Deconvoluted peak showing the presence of BCC and B2 phase after SPS.	84
Figure 4.9	Back-scattered SEM micrograph showing coarse and fine microstructure of spark plasma sintered MgAlSiCrFeNi HEA in (a) and (b) respectively. (c) and (d) shows the area and points for area and point EDS analysis respectively. (e) EDS spectrum corresponding to the full area scanning.	85
Figure 4.10	SEM – EDS elemental mapping showing distribution of elements in spark plasma sintered MgAlSiCrFeNi HEA.	86
Figure 4.11	(a) Plot showing indentation load vs depth of indentation; (b) SEM micrograph showing the indentation mark at a load of 5000 mN; (c) radar diagram for mechanical property of MgAlSiCrFeNi LDHEA SPSed at 800 °C (1073K) for 15 min.	88
Figure 5.1	Phase evolution after mechanical alloying of MgAlSiCrFeCuZn HEA up to 50 h with BPR of 10:1 (a); Enlarged image showing peak position of (110) peak of BCC and minor phase in 50 h milled powder (b); Deconvoluted peak showing the presence of BCC and γ -brass type phase in 50 h milled powder (c).	98
Figure 5.2	Phase evolution during mechanical alloying of MgAlSiCrFeCuZn HEA up to 50 h with BPR of 20:1.	99
Figure 5.3	Variation of crystallite size and lattice strain as function of milling duration.....	100
Figure 5.4	TEM micrograph showing fine microstructural details of 50 h milled powder. (a), (b), (c) representing BF, SAD pattern and DF images showing presence of BCC phase; (d), (e) and (f) representing BF, composite SAD pattern and DF images showing co-existence of BCC and γ -brass type phase; (g) and (h) represents BF and SAD pattern of powder particle having only γ -brass type phase; (i) and (j)	

	represents BF and SAD pattern of severely deformed powder particles having BCC phase.....	101
Figure 5.5	STEM-EDS mapping of 50 h milled HEA powder particle.	102
Figure 5.6	SEM micrograph showing morphology of 30 h (a & d), 40 h (b & e) and 50 h (c & f) milled powder.	104
Figure 5.7	Particle size distribution of 50 h mechanically alloyed MgAlSiCrFeCuZn LDHEA with a BPR of 10:1 and 20:1.	105
Figure 5.8	DSC thermogram of 50 h milled powder up to 1000 °C (1273 K) with scan rate of 20 k.min ⁻¹	106
Figure 5.9:	Ex-situ XRD of 50 h mechanically alloyed MgAlSiCrFeCuZn LDHEA powder annealed at various temperatures up to 1000 °C (1273 K).....	107
Figure 5.10	Phase formation in MgAlSiCrFeCuZn HEA powder spark plasma sintered at 800 °C (1273 K) for 15 min (a); Enlarged image showing the peak position of BCC/ B2 phase along with other minor phases (b); Expanded image of the deconvoluted peaks for BCC/ B2 phase along with other minor phases (c).....	108
Figure 5.11	Plot showing Indentation load vs depth of indentation for MgAlSiCrFeCuZn LDHEA powder spark plasma sintered at 800 °C (1273 K) for 15 min.	109

List of Tables

		<i>Page No.</i>
Table 1.1	Classification of various metallic systems based on ΔS_{conf}	5
Table 1.2	Diffusion indices for Ni in various FCC matrices. The compositions of Fe-Cr-Ni (Si) alloy are given in wt.%.....	8
Table 1.3	Enthalpy matrix relevant to the Al-Li-Mg-Sc-Ti alloy (in kJ/m).	21
Table 1.4	Typical range of hardness values in HEAs based on their phase evolution.....	27
Table 2.1	Basic properties of the selected elements for the study.....	38
Table 2.2	Nominal (atomic %) compositions of milled alloys.....	38
Table 2.3	Parameters for milling utilized in the production of HEA powder.....	38
Table 3.1	Elemental composition of spark plasma sintered MgAlSiCrFe HEA.....	55
Table 3.2	Density and mechanical properties of SPSed MgAlSiCrFe HEA.....	56
Table 3.3	Physiochemical parameters and enthalpy of mixing of constituent elements in MgAlSiCrFe HEA.....	58
Table 3.4	Calculated thermodynamic and physical parameter of MgAlSiCrFe HEA.....	59
Table 3.5	Single point equilibrium calculation is done to estimate phase fraction and phase composition as a function of temperature.....	63
Table 4.1	Variation of crystallite size (nm), lattice strain (%) and dislocation density along with milling time for MgAlSiCrFeNi HEA.....	73
Table 4.2	Elemental composition of MgAlSiCrFeNi milled HEA powder for 60 h.....	78
Table 4.3	Elemental composition of MgAlSiCrFeNi HEA SPSed sample.....	89
Table 4.4	Density and mechanical properties of SPSed MgAlSiCrFeNi LDHEA.....	90
Table 4.5	Physical data of constituent elements in MgAlSiCrFeNi HEA.....	91
Table 4.6	Enthalpy of mixing (kJ/mol) of binary elements in MgAlSiCrFeNi HEA by semi-empirical Miedema's approach.....	93
Table 4.7	Calculated thermodynamic and other parameter of MgAlSiCrFeNi HEA.....	95

Table 5.1	Variation of crystallite size and lattice strain of MgAlSiCrFeCuZn MA high entropy alloy.....	100
Table 5.2	Mechanical properties of SPSed MgAlSiCrFeCuZn LDHEA.....	103
Table 5.3	Chemical enthalpy of mixing (ΔH_{ij}^{mix} , kJ/mol) of atomic pairs for MgAlSiCrFeCuZn LDHEA following the Miedema's approach.....	111

Abbreviations

HEA	: High Entropy Alloy
RHEA	: Refractory HEA
LDHEA	: Low-Density HEA
LWHEA	: Light Weight HEA
YS	: Yield Strength
IM	: Intermetallics
XRD	: X-ray Diffraction
BPR	: Ball to Powder Ratio
SE	: Secondary Electron
MA	: Mechanical Alloying
SPS	: Spark Plasma Sintering
HIP	: Hot Isostatic Pressing
VIM	: Vacuum Induction Melting
HEBM	: High Energy Ball Milling
BSE	: Back-Scattered Electron
CCA	: Complex Concentrated Alloy
SEM	: Scanning Electron Microscopy
ODS	: Oxide Dispersion Reinforced
EDS	: Energy Dispersive X- ray Spectroscopy
DSC	: Differential Scanning Calorimetry
VEC	: Valence Electron Concentration
VHP	: Vacuum Hot Pressing and Sintering
TEM	: Transmission Electron Microscopy
ICDD	: International Centre for Diffraction Data
LWEFM	: Light Weight Environmentally Friendly Materials

Symbols

k	:	Boltzmann constant
S	:	Configurational entropy
W	:	Number of possible configurations
ΔS_{conf}	:	Change in configurational entropy
R	:	Gas constant
ΔG_{mix}	:	Gibbs free energy change due to mixing
δ	:	Atomic size difference
ΔH_{mix}	:	Enthalpy of mixing
ΔS_{mix}	:	Entropy of mixing
T_m	:	Melting point
σ	:	Sigma phase
σ_y	:	Yield stress
M_s	:	Saturated magnetization
χ	:	Permeability
λ	:	Wave length
β	:	Peak broadening
t	:	Crystallite size

PREFACE

The engineering materials used for various applications generally consist of one or two major elements along with other minor alloying elements for improving the mechanical and functional properties. Over the years, the paradigm shifts in alloy design and development strategies has led to the discovery of various new classes of advanced materials for engineering applications such as composites, quasicrystals, bulk metallic glasses and more recently the multi-component high entropy alloys, among other materials.

The new categories of alloys emerging on the concept of alloys with multiple principal elements are referred to as High Entropy Alloys (HEAs). The early conceptualizations of equimolar alloys date back to late 1700s in a book written in French by Karl Franz Achard. He described the idea of equimolar alloys having five to seven elements. However, in the modern days the first report on multi-component HEAs was published independently by Brian Cantor and J.W. Yeh in the year of 2004. The term ‘High Entropy Alloys’ was first coined by J.W. Yeh and he described HEAs as multi-principal alloys containing five or more elements with equiatomic or near-equiatomic atomic fraction in the range of 5-35 at%. In the recent years, D. B. Miracle & co-workers classified these HEAs into three broad categories, i.e. (i) transition metal based HEAs, (ii) refractory metal based HEAs and (iii) low-density metal based HEAs. The transition metal-based HEAs are made up of mostly transition metals. The elements like Ti, V, Cr, Nb, Mo, Hf, Ta, and W are used as major elements to develop refractory HEAs. For developing low density high entropy alloys (LDHEAs) normally lighter elements like Li, Be, Mg, Al, Si, Sc etc. are selected as the major components.

The present work is focused on the phase evolution, microstructural features, thermal stability and mechanical properties of three LDHEAs such as MgAlSiCrFe, MgAlSiCrFeNi and MgAlSiCrFeCuZn, which were processed by mechanical alloying (MA) and spark plasma sintering (SPS) techniques. The present thesis is organized into of six chapters.

Chapter 1: The first chapter gives a brief introduction of the HEAs and basic principles of their stability. This chapter discusses the phase prediction rules for the design and development of HEAs and the core effects. Additionally, this chapter provides the literature survey of the processing methods for HEAs. Various kinds of possible phases that can form in HEAs and its influence on the properties of these HEAs are elaborated. A brief discussion about the low-density HEAs (LDHEA) is also included. The motivation and objectives of the present studies has been highlighted at the end of this chapter.

Chapter 2: The second chapter of this thesis deals with the materials and experimental techniques that were employed in the preparation of the LDHEAs. The synthesis of LDHEAs by mechanical alloying (MA) and its consolidation using spark plasma sintering (SPS) with details on the parameters and operational protocol have been described. Various characterization techniques such as X-ray diffraction (XRD), transmission electron microscopy (TEM) and scanning electron microscopy (SEM) adopted for characterizing microstructure and structures of the phases are mentioned. The nominal chemical composition of the LDHEA powder and of consolidated samples were investigated using SEM equipped with EDS (energy dispersive x-rays spectroscopy) detector. The chemical composition and elemental distribution of the nanostructured powders were further analysed by STEM-EDS techniques. The thermal stability of the milled powders were evaluated through differential scanning calorimetry (DSC) and ex-situ XRD of the annealed milled powders. The experimental determination of density and hardness of the sintered samples (using conventional and instrumented indentation techniques) were described briefly.

Chapter 3: The third chapter of this thesis examines an equiatomic MgAlSiCrFe HEA prepared by using mechanical alloying. This chapter discusses the alloying behavior, phase evolution, phase composition, and thermal stability of as-milled nanostructured HEA powders. The milling of elemental powders of MgAlSiCrFe for 60 h led to the formation of HEA having

BCC phase with a lattice parameter of 0.2887 ± 0.005 nm (close to that of the α -Fe) along with a minor fraction of undissolved Si. The nanostructured HEA powders having crystallite size of ~ 19 nm was observed to form after milling. The STEM–EDS mapping of these milled powders confirmed uniform elemental distribution in the sample milled for 60 h. The DSC thermogram of 60 h milled HEA powder demonstrated its thermal stability up to 400 °C. The exothermic heating events detected in the DSC thermogram corresponded to the phase transformation of MgAlSiCrFe LDHEA powder. Attempts have been made to corroborate these observation with the results obtained in ex-situ XRD analysis of the powders annealed at various temperatures up to 700 °C. The systematic investigation established the presence of parent BCC phase along with other minor phase's i.e. B2 type Al–Fe phase, FCC phases (Al–Mg solid solution), Cr_5Si_3 , Mg_2Si , and $\text{Al}_{13}\text{Fe}_4$. Additionally, this chapter correlates the experimental results with the thermodynamic parameters in order to understand the phase evolution and stability. This chapter also shows the phase evolution, chemical composition, and microstructure of the SPSed sample consolidated at 800 °C (1073 K) through XRD and SEM techniques. The SPSed samples revealed the formation of B2-type AlFe phase ($a=0.2889$ nm) along with the parent disordered BCC phase and a minor fraction of $\text{Al}_{13}\text{Fe}_4$, β - Al_3Mg_2 , and Cr_5Si_3 phases. The instrumented microindentation techniques was used to examine the mechanical properties of these LDHEAs. The hardness, Young's modulus and yield strength were found to be approximately 7.42 ± 0.18 GPa, 212 ± 2 GPa and 2.47 GPa with an appreciable relative density of 99.98% for the SPSed samples. This chapter also describes the phase evolution using Thermo-Calc software, the thermodynamic parameters and property diagrams which were generated through the CALPHAD approach.

Chapter 4: The fourth chapter of this thesis deals with the equiatomic MgAlSiCrFeNi LDHEA prepared by mechanical alloying followed by spark plasma sintering (SPS). In this chapter, the phase evolution, chemical composition, and thermal stability of the alloy were

analyzed. The formation of a BCC phase with lattice parameter of 0.2876 ± 0.03 nm and along with undissolved Si (~ 3 at%) was observed after 60 h of milling. The DSC experiment up to 1200 °C (1473 K) showed five exothermic heating events corresponding to the various phase transformations, which were further correlated with the results obtained from the XRD experiments. This chapter reports various phase transformation events due to annealing at different temperature upto 800 °C (1073 K) resulting in the formation of a major B2 type phase ($a=0.289$ nm) and BCC phase along with small amounts of FCC Al-Mg solid solution phase (FCC 1 ($a=0.4082$ nm) and FCC 2 ($a=0.4215$ nm)), and intermetallic phases such as monoclinic $\text{Al}_{13}\text{Fe}_4$ ($a=1.549$ nm, $b=0.808$ nm, $c=1.248$ nm, $\alpha=\beta=90^\circ$), Mg_2Si ($a=0.6351$ nm), Cr_5Si_3 ($a=b=0.9165$ nm, $c=0.4638$ nm). The SPSed sample also exhibited BCC and B2-type phases coexisting with the minor amount of other phases observed for 800 °C (1073 K) annealed sample. It has been further observed that the co-existence of minor phases along with the parent BCC phase in SPSed alloy (having a relative density of $\sim 99.40\%$) led to high hardness and modulus of elasticity of $\sim 9.98 \pm 0.3$ GPa and 229 ± 0.3 GPa respectively. The present chapter also focuses on calculating thermodynamic parameters in order to correlate the experimental findings of phase evolution and stability of the annealed powder as well as SPSed samples.

Chapter 5: The fifth Chapter of this thesis deals with equiatomic septenary MgAlSiCrFeCuZn LDHEA synthesized by mechanical alloying for 60 h followed by spark plasma sintering. The phase evolution, powder morphology, chemical composition and thermal stability of the 60 h milled HEA powder was ascertained. The mechanical alloying led to the formation of a major BCC phase (lattice parameter of 0.2895 nm) with the minor fraction of retained Si. The thermal stability of the milled powders were discerned through the DSC thermogram upto 1200 °C (1473 K) and the various exothermic heating events were corroborated with the phases observed in the ex-situ XRD of annealed powders. The MgAlSiCrFeCuZn HEA was consolidated at 800 °C using spark plasma sintering. The hardness and yield strength of

conventionally sintered and SPSed samples were determined using instrumented indentation techniques. The hardness and modulus was found to be ~8.38 GPa and 211 GPa. The excellent indentation hardness is understood due to the appreciable density achieved in the SPSed samples. The present chapter also focuses on calculating thermodynamic parameters, in order to correlate with the experimental findings of phase evolution and stability of the annealed powder and SPSed samples.

Chapter 6: The sixth chapter provides a summary of the work, highlighting the important findings and significant results arising from the present thesis. It has also addressed the suggestions for future work in the areas of LDHEAs required for further understanding.

References: This section contains a list of pertinent references more than one hundred and fifty publications that have been refereed while discussing the various aspects of the issues related to the present thesis.